International Journal of GEOMATE, May 2019, Vol.16, Issue 57, pp.176 - 182
Geotec., Const. Mat. & Env., DOI: https://doi.org/10.21660/2019.57.8323
ISSN: 2186-2982 (Print), 2186-2990 (Online), Japan

SEISMIC MICROZONATION OF SEMARANG, INDONESIA, BASED ON PROBABILISTIC AND DETERMINISTIC COMBINATION ANALYSIS

*Windu Partono[1], Masyhur Irsyam[2], I Wayan Sengara[2] and Muhammad Asrurifak[3]

[1]Faculty of Engineering, Diponegoro University, Indonesia; [2] Faculty of Civil and Environmental Engineering, Bandung Institute of Technology, Indonesia; [3]Research Center for Disaster Mitigation, Bandung Institute of Technology, Indonesia

*Corresponding Author, Received: 30 Oct. 2018, Revised: 20 Dec. 2018, Accepted: 11 Jan. 2019

ABSTRACT: One of the most important pieces of information obtained from the new Indonesian seismic hazard maps completed in 2017 was the identification of a fault that crosses the city of Semarang. This fault can be categorized as a new dangerous seismic source and should be taken into account in future seismic mitigation planning of this city. This paper describes the seismic microzonation of Semarang carried out via a combination of probabilistic and deterministic hazard analysis. The purpose of this research was to develop a risk map for Semarang based on one percent building collapse in 50 years. The analysis was performed using the same method employed in developing risk targeted Maximum Considered Earthquake (MCE_R) maps in 2012, with an improved beta (logarithmic standard deviation) value of 0.65 and adjusted direction factors of 1.1 and 1.3 for short- and long-period spectral acceleration, respectively. Whereas the 2012 maximum MCE_R spectral acceleration was distributed in the north-east of the study area due to the presence of Lasem fault, the 2018 maximum is located in the north-western part of the city as a result of the newly developed Semarang fault.

Keywords: Seismic microzonation, Fault, Probabilistic, Deterministic, MCE_R

1. INTRODUCTION

The new Indonesian seismic hazard maps were developed in 2017 by the National Center for Earthquake Studies [1]. All maps were produced based on probabilistic seismic hazard analysis (PSHA). Eight different maps with varying probabilities of exceedance, ranging from 20% probability of exceedance in 10 years (50-year of return period) through to 1% probability of exceedance in 100 years (10000-year return period). Major improvements were made regarding historical earthquakes data, earthquake fault assessment data and seismotectonic map data, and minor improvements in ground motion prediction equations [2]. One of the most important seismic hazard maps used in developing the Indonesian Seismic Code for Building Resistance is the 2500-year return period seismic hazard map (2% probability of exceedance in 50 years).

However, the development of new seismic hazard maps for building design remains on-going and following the same procedures implemented in developing the 2012 Indonesian seismic code for building and other structure design [3]. The new seismic hazard maps for Indonesian Seismic Code are being developed using a combination of probabilistic (2% probability of exceedance in 50 year) and deterministic hazard analysis, as well as risk targeted ground motion (RTGM) analysis of probabilistic seismic hazard to determine 1% probability of building collapse in 50 years [3, 4]. The new RTGM analysis includes modified beta (β), logarithmic standard deviation, values and a modified of direction factor for 0.2 seconds and 1-second spectral acceleration. RTGM analysis is being applied to the whole area of the country from East longitude 94^o to 142^o and from North latitude 8^o to South latitude 12^o with 0.1-degree grid spacing on both directions longitude and latitude.

As part of this research, a combination of probabilistic and deterministic seismic hazard analysis is to be implemented for developing maximum considered earthquake (MCE) for the whole area of the country. Three risked targeted maximum considered earthquake ground motion (MCE_R) maps, Peak ground acceleration (PGA), short period (0.2 seconds) and long period (1 second), are developed for the whole area of Indonesian country.

This paper describes the development of seismic microzonation of Semarang, Indonesia, by conducting a combination of probabilistic and deterministic seismic hazard analysis in the development of three MCE_R maps (MCES for the 0.2-second period, MCES1 for the 1-second period and MCEG for peak ground acceleration). Seismic

microzonation of the city was implemented on 288 borehole locations by conducting weighted interpolation of the four closest points of the national MCES, MCES1 and MCEG result calculations. All borehole investigations were conducted during the period from 2009 until 2017 at a minimum of 30 m depth. Average shear wave velocity (V_S30) were previously calculated using standard penetration test data (N-SPT) and conducting three empirical formulas proposed by [5], [6] and [7]. A comparative analysis was then carried out in this study to evaluate all MCES and MCES1 values calculated at 288 borehole locations based on 2018 and 2012 data. Fig. 1 shows a V_S30 map of Semarang, the borehole locations and two fault traces (Semarang and Lasem fault).

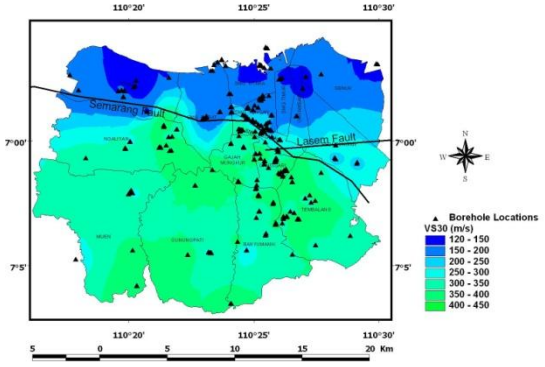

Fig.1 V_S30 map of Semarang, borehole locations and two fault traces

2. SEISMIC HAZARD ANALYSIS

2.1 Seismotectonic Data

Major improvements to the seismotectonic data for the Semarang region were made for seismic hazard analysis. Seismotectonic data for the year 2010 seismic hazard analysis are dominated by 5 (five) shallow crustal fault sources (Cimandiri, Lembang, Yogya, Lasem, and Opak) and 1 (one) subduction source (Java Megathrust). In contrast, the 2017 seismic hazard analysis data [1] are characterized by 8 (eight) shallow crustal fault data (Cimandiri, Lembang, Baribis-Kendeng, Ciremai, Ajibarang, Opak, Merapi-Merbabu and Pati) clearly identified and located within a 500 Km radius of Semarang. The eight shallow crustal fault data can be divided into 26 (twenty-six) fault segments. Table 1 displays the seismotectonic data for the 26 fault segments used for seismic hazard analysis. Seismic parameters SR, SM, D, M, RS and SS in this table represent the slip rate (mm/year), seismic mechanism, dip (degree), the maximum magnitude (Mw), reverse-slip and strike-slip, respectively.

In the 2017 seismic hazard analysis, 1 (one) subduction source (Java Megathrust) was clearly identified and located on the southern part of Java island. For further 2018 seismic hazard analysis, Java subduction megathrust source can be divided into two segments: West and Central-East Java. Table 2 displays all parameter data used to analyze the Java subduction megathrust source, where L, W, SR and M stand for length (Km), width (Km), slip rate (cm/year) and maximum magnitude (Mw), respectively. Fig. 2 shows the seismotectonic map of Java Island used in PSHA development; the fault numbers displayed in Fig. 2 are related to the segment fault number listed in Table 1.

Table 1 Shallow crustal fault parameter data [1]

No	Fault Segments	SR	SM	D	M
1	Cimandiri	0.55	RS	45	6.7
2	Cibeber	0.40	RS	45	6.5
3	Rajamandala	0.1	SS	90	6.6
4	Lembang	2.0	SS	90	6.8
5	Subang	0.1	RS	45	6.5
6	Cirebon-1	0.1	RS	45	6.5
7	Cirebon-2	0.1	RS	45	6.5
8	Karang Malang	0.1	RS	45	6.5
9	Brebes	0.1	RS	45	6.5
10	Tegal	0.1	RS	45	6.5
11	Pekalongan	0.1	RS	45	6.5
12	Weleri	0.1	RS	45	6.5
13	Semarang	0.1	RS	45	6.5
14	Rawapening	0.1	RS	45	6.5
15	Demak	0.1	RS	45	6.5
16	Purwodadi	0.1	RS	45	6.5
17	Cepu	0.1	RS	45	6.5
18	Waru	0.05	RS	45	6.5
19	Surabaya	0.05	RS	45	6.5
20	Blumbang	0.05	RS	45	6.6
21	Ciremai	0.1	SS	90	6.5
22	Ajibarang	0.1	SS	90	6.5
23	Opak	0.75	SS	60	6.6
24	Merapi-Merbabu	0.1	SS	90	6.6
25	Pati	0.1	SS	90	6.5
26	Lasem	0.5	SS	90	6.5

Table 2 Subduction parameter data [1]

No	Segment	L	W	SR	M
1	West	320	200	4.0	8.8
2	Central-East	400	200	4.0	8.9

Seismic hazard analysis was performed using earthquake data covering the period from 1901 to

2014 [2] collected from the Meteorological Climatological and Geophysical Agency (BMKG) with focal mechanism from the International Seismological Commission (ISC) databases, the EHB catalogue and Preliminary Determination of Epicenters (PDE) [2]. All hypocenter earthquake data have been relocated to the correct positions [2].

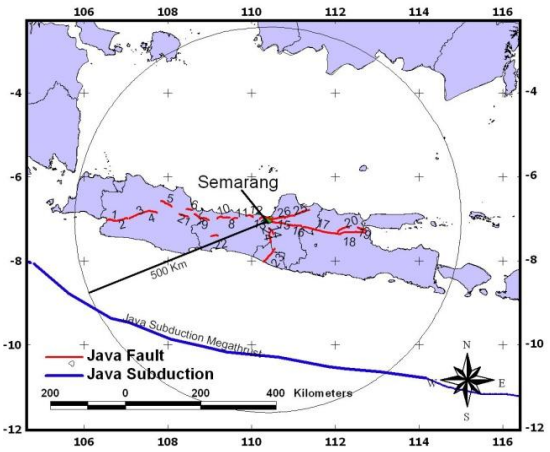

Fig.2 Seismotectonic map of Java Island

2.2 Ground Motion Prediction Equations

The selection of an appropriate ground motion prediction equation (attenuation function) is essential for calculating or predicting spectral acceleration at a specific site. Following the same method implemented for the 2010 Indonesian seismic hazard maps, all attenuation function used for the 2017 seismic hazard maps were divided into four different seismic source mechanism: shallow crustal fault, shallow background, subduction megathrust (Interface) and deep background (Benioff). Compare to the 2010 seismic hazard maps, a minor improvement in attenuation function was applied for the 2017 seismic hazard maps, with a new attenuation function employed especially for the subduction interface [8] to replace attenuation function [9]**.** Table 3 shows all attenuation functions used in developing the 2017 Indonesian seismic hazard maps.

2.3 Probabilistic and Deterministic Hazard Analyses

Both seismic hazard analyses, probabilistic (PSHA) and deterministic (DSHA), were performed to obtain spectral acceleration at bedrock elevation. PSHA was implemented using the total probability theorem [15]. Eq. (1) shows the basic formula to obtain the total average rate of exceedance of an earthquake (λa^*) with an acceleration greater than the specific acceleration value a*. P_m (m) and $P_r(r)$ in this equation represent the probability distribution function for magnitude (m) and distance (r), respectively and v represents the mean rate of exceedance. DSHA was implemented using 84th percentile, equal to 180% of median spectral acceleration.

Table 3 Attenuation functions used for developing 2017 seismic hazard maps

Seismic Mechanism	Attenuation Functions
Shallow Crustal Fault	[10] - [12]
Shallow Background	[10] - [12]
Interface Megathrust	[8], [13], [14]
Benioff Subduction Intraslab	[9], [14]

$$\lambda a^* = v \int_m \int_r (Pa > a^* | m,r) P_m(m) P_r(r) dr\, dm \qquad (1)$$

Following the same steps conducted in developing the 2010 national seismic hazard maps and 2012 national seismic code [3], integration of PSHA and DSHA was implemented to develop new 2018 MCE_R maps for the entire territory of Indonesia. MCE_R values were calculated by combining risk targeted ground motion analysis (RTGM) for a 1% probability of collapse in 50 years and 84th percentile deterministic seismic hazard analysis, with adjusted direction factors of 1.1 for 0.2 second period and 1.3 for 1 second period spectral acceleration, and conducting β (logarithmic standard deviation) equal to 0.65. The 2012 seismic code used a β value equal to 0.7, direction factors of 1.05 and 1.15 for short-period and long-period spectral acceleration, respectively. Eq. (2) and Eq. (3) express the log-normal distribution functions of building collapse capacity [3, 4] used in developing the RTGM maps, with 'c' representing spectral acceleration and $c_{10\%}$ the 10th percentile collapse capacity.

$$f_F(c) = \frac{1}{c\beta\sqrt{2\pi}} \exp\left[-\frac{\ln c - (\ln c_{10\%} + 1.28\beta)^2}{2\beta^2} \right] \qquad (2)$$

$$P[collaps] = \int_0^\infty f_F(c)\, P[S > c]\, dc \qquad (3)$$

The schematic approach employed in combining PSHA and DSHA was first illustrated by [16], with this model adopted in the present study to calculate the MCE_R values (2018). Fig. 3 shows the graphical procedure used in developing the new 2018 MCE_R values based on combining

RTGM and 84th percentile deterministic seismic hazard [3, 16 and 17].

Seismic microzonation of Semarang was carried out based on the obtained national MCE_R analysis results by combining risk targeted ground motion analysis (RTGM) for a 1% probability of collapse in 50 years and 84th percentile deterministic seismic hazard analysis with an adjusted direction factor of 1.1 for 0.2 second period and 1.3 for 1 second period spectral acceleration.

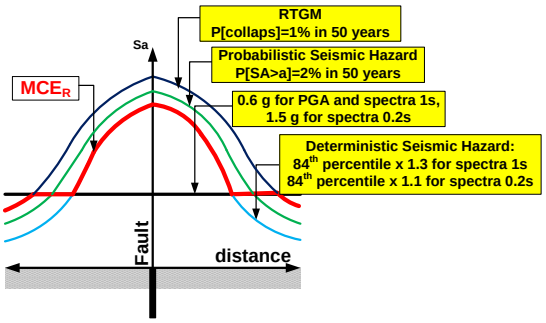

Fig.3 MCE_R 2018 design procedure

The analysis at 288 borehole locations was performed by conducting weighting interpolation for each borehole location to the four closest positions of national MCE_R data. MCE_R (MCEG, MCES, and MCRS1) values at each borehole location were interpolated using Eq. (4) and Eq. (5), where M_b represents MCE_R value at each borehole location. Mi is the national MCE_R value at point 'i' where i = 1 to 4, 'di' represents the minimum distance from borehole location to point number 'i' and 'wi' is weight factor of each borehole location to point number 'i'.

$$wi = \frac{1/di}{\sum_{i=1}^{4} 1/di} \quad (4)$$

$$M_b = \sum_{1}^{4} (wi * Mi) \quad (5)$$

3. RESULTS AND DISCUSSIONS

The analysis of MCEG, MCES, and MCES1 were performed at 288 borehole locations. Fig. 4, 5 and 6 show the produce 2018 MCEG, MCES and MCES1 maps, respectively. As can be seen in Fig. 4 and Fig. 5 maximum MCEG and MCES spectral acceleration values were identified in the western part of the city, with maximum MCEG are 0.45 g and maximum MCES is 0.95 g (g is gravitational acceleration). As can be seen in Fig. 6, the MCES1 values ranging between 0.35 g to 0.4 g are identified across the whole part of the city.

MCEG, MCES and MCES1 distributions in terms of V_S30 (i.e. their correlation) were applied for all 288 borehole locations. The purpose of the analysis is to obtain the correlation between V_S30 and MCEG, MCES and MCES1 values. The V_S30 value was implemented in the present study due to the important correlation between V_S30 and site class in developing surface spectral accelerations [17].

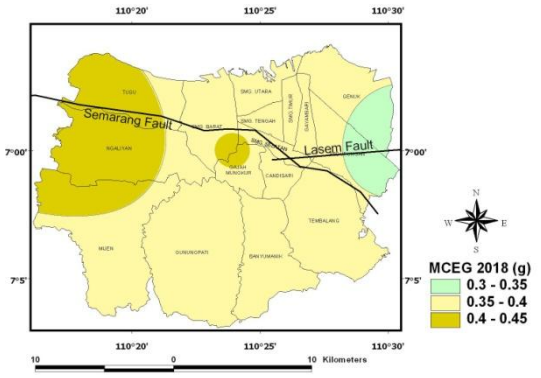

Fig.4 MCEG 2018 map for Semarang

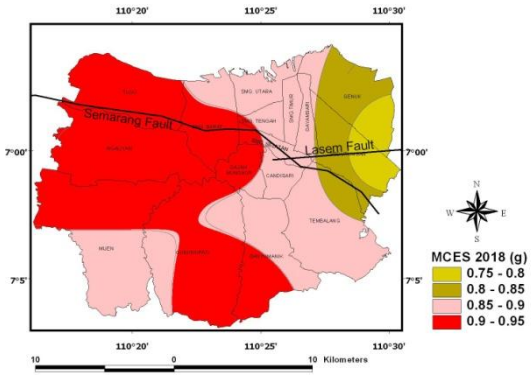

Fig.5 MCES 2018 map for Semarang

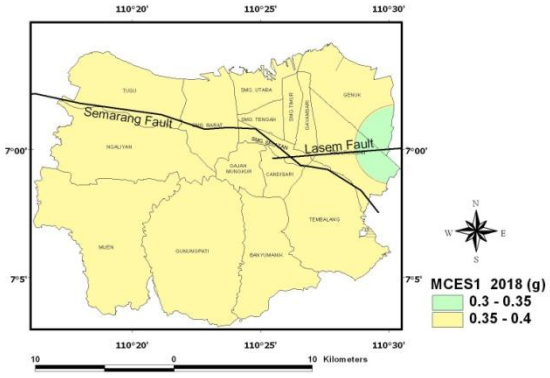

Fig.6 MCES1 2018 map for Semarang

The distributions of MCE_R 2018 values (MCEG, MCES and MCES1) at the 288 borehole locations were thus developed based on V_S30 values producing the scatter distribution chart shown in Fig. 7. Analysis of this figure clearly reveals that MCEG, MCES and MCES1 show to a slight increase with increasing V_S30 values from 120 m/s to 420 m/s. Table 4 displays the distribution of average MCE_R (2018) values in terms of V_S30 and site soil class [18], where SE, SD and SC on this table represent soft, medium and hard soil, respectively.

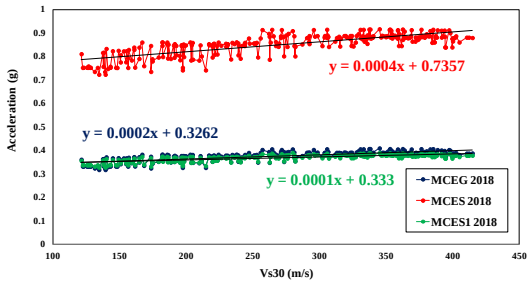

Fig.7 MCEG, MCES and MCES1 (2018) distribution in terms of V_S30

Table 4 Average MCEG, MCES and MCES1 (2018) values

V_S30 (m/s)	Site Class	MCEG (g)	MCES (g)	MCES1 (g)
<175	SE	0.35	0.78	0.35
175 - 350	SD	0.38	0.86	0.37
350 - 750	SC	0.39	0.88	0.38

Comparative analysis was then undertaken between 2012 and 2018 MCES and MCES1 values at 288 borehole locations. The purpose of the analysis is to obtain the difference between 2012 and 2018 MCES and MCES1 distribution in Semarang. Fig. 8 shows the distribution of 2012 MCES values and Fig. 9 shows the distribution of 2012 MCES1 values. As it can be seen in Fig. 8 the maximum 2012 MCES values were identified on the eastern part of the city with maximum of 1.4 g. Maximum 2012 MCES1 values were identified in the small eastern part of the study area with maximum of 0.5 g.

The difference between 2018 and 2012 MCES and MCES1 distribution values in terms of V_S30 is depicted in Fig. 10 and Fig. 11, respectively. Fig. 10 shows the difference between MCES (2018) and MCES (2012) values. As can be seen on this figure average MCES (2012) values are relatively greater than in MCES (2018) values. Table 5 shows the improvement of MCES values. As can be seen on this table the MCES (2018) is 84.33% to 86.41% lower than in MCES (2012) values.

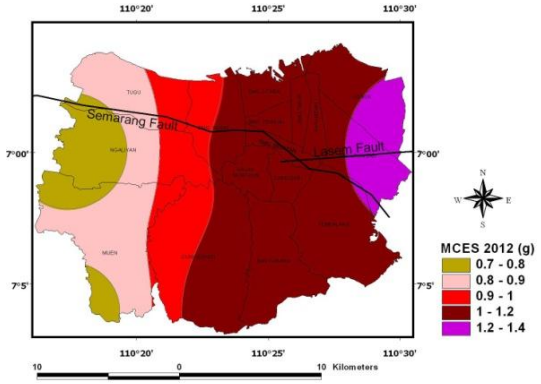

Fig.8 MCES 2012 map of Semarang

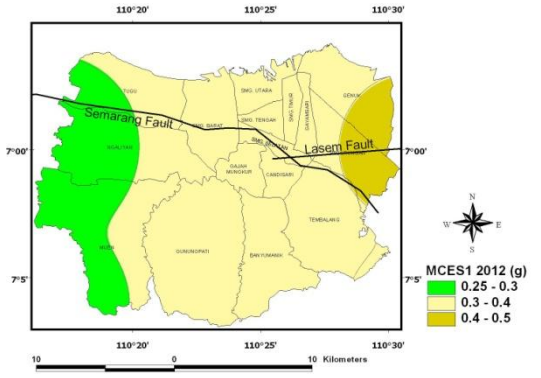

Fig.9 MCES1 2012 map of Semarang

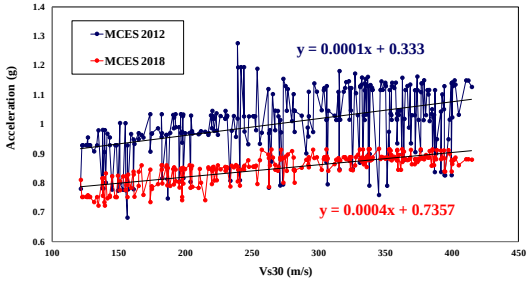

Fig.10 MCES 2018 and MCES 2012 distributions in terms of V_S30

Table 5 The difference between MCES (2018) and MCES (2012)

V_S30 (m/s)	MCES (2012) (g)	MCES (2018) (g)	+ / -
<175	0.90	0.78	-86.41%
175 - 350	1.02	0.86	-84.33%
>350	1.04	0.88	-84.93%

+: increase; -: decrease

Fig. 11 shows the difference between MCES1 (2018) and MCES1 (2012) values. As can be seen in this figure the MCES1 (2012) values are relatively smaller than in MCES1 (2018) values. Table 6 shows the improvement of MCES1 values. As can be seen on this table the MCES (2018) is 108.21% to 110.79% greater than in MCES1 (2012).

All MCES values in Table 5 and MCES1 values in Table 6 are divided into three different V_S30 categories which representing three different site soil classes [18]. Based on Fig 10 and Fig 11, MCES and MCES1 values exhibit a positive linear relationship with V_S30 values. All MCES and MCES1 2018 and 2012 values are calculated at 288 borehole locations.

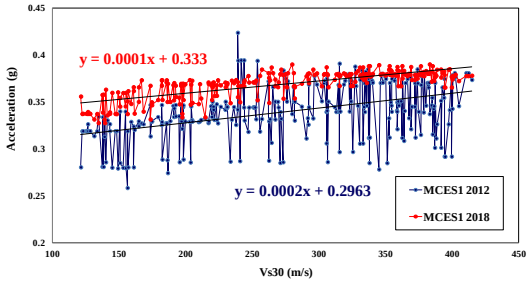

Fig.11 MCES1 (2018) and MCES1 (2012) distributions in terms of V_S30

Table 6 The difference between MCES1 (2018) and MCES1 (2012)

V_S30 (m/s)	MCES1 (2012) (g)	MCES1 (2018) (g)	+ / -
<175	0.31	0.35	+110.79%
175 - 350	0.34	0.37	+108.21%
>350	0.35	0.38	+108.29%

+: increase; -: decrease

4. CONCLUSIONS

Seismic microzonation of Semarang, Indonesia, was implemented based on the combination of probabilistic and deterministic seismic hazard analyses. Risk targeted ground motion (RTGM) analysis was conducted using a β value of 0.65 and adjusted direction factors of 1.1 for 0.2 second period spectral acceleration and 1.3 for 1 second period spectral acceleration was implemented in this study. The purpose of this study was to evaluate the distribution of maximum considered earthquake (MCE_R) values across Semarang based on the new 2017 seismic hazard maps. Comparative analysis was then undertaken with MCE_R (2012) values, which were used previously in the development of the 2012 Indonesian seismic code.

Maximum 2018 MCE_R (MCES and MCES1) values for Semarang are distributed in the north-western part of the city at a maximum of 0.45 g for MCEG, 0.95 g for MCES and 0.4 g for MCES1. This pattern is the opposite of that identified in 2012 MCE_R distribution values, with 2012 MCES and MCES1 maximum are identified on the north-eastern part of the city.

Comparative analysis was also implemented in this study by comparing 2018 and 2012 MCE_R values. The analysis was performed for MCES and MCES1 values at 288 borehole locations. On average, the MCES (2018) values are 84.33% to 86.41% lower than the MCES (2012) values. However the MCES1 (2018) values are 108.21% to 110.79% greater than the MCES1 (2012) values.

5. ACKNOWLEDGMENTS

The authors would like to thank the Ministry of Public Works and Human Settlements Indonesia and National Center for Earthquake Studies for providing data and technical supports during the development of this study.

6. REFERENCES

[1] Pusat Studi Gempa Nasional, Peta Sumber Dan Bahaya Gempa Indonesia Tahun 2017, Pusat Litbang Perumahan dan Pemukiman, Kementerian Pekerjaan Umum dan Perumahan Rakyat (National Center for Earthquake Studies, Indonesian Seismic Sources and Seismic Hazard Maps 2017, Centre for Research and Development of Housing and Resettlement, Ministry of Public Works and Human Settlements), ISBN 978-602-5489-01-3, 2017, pp. 1-377.

[2] Irsyam M., Hendriyawan, Natawijaya D.H., Daryono M.R., Widiyantoro S., Asrurifak M., Meilano I., Triyoso W., Hidayati S., Rudiyanto A., Sabarudin A. and Faisal L., Development of new seismic hazard maps of Indonesia, Proceedings of the 19th International Conference on Soil Mechanics and Geotechnical Engineering, Seoul, 2017, pp. 1525-1528.

[3] Sengara I.W., Irsyam M., Sidi I.D., Mulia A., Asrurifak M. and Hutabarat D., Development of Earthquake Risk-Targeted Ground Motions for Indonesian Earthquake Resistance Building Code SNI 1726-2012, Proceedings of the 12th International Conference on Applications of Statistics and Probability in Civil Engineering,

ICASP12, Vancouver Canada , July 12-15, 2015, ISBN 978-0-88865-245-4.

[4] Luco N., Ellingwood B.R., Hamburger R.O., Hooper J.D., Kimbal J.K. and Kircher C.A., Risk-Targeted versus current seismic design maps for the conterminous United States, Structural Engineers Association of California 2007 Proceedings, 2007, pp. 163-175.

[5] Ohsaki Y. and Iwasaki R., On dynamic shear moduli and Poisson's ratio of soil deposits, Soils and Foundations, Vol. 13 (4), 1973, pp. 59-73.

[6] Ohta Y. and Goto N., Empirical Shear Wave Velocity Equations in terms of characteristic soil indexes, Earthquake Engineering and Structural Dynamics, Vol. 6, 1978, pp. 167-187.

[7] Imai T. and Tonouchi K., Correlation of N-Value with S-Wave velocity and Shear Modulus, Proceedings of Second European Symposium on Penetration Testing, Amsterdam, The Netherlands, 1982, pp. 67-72.

[8] Abrahamson N.A., Gregor N. and Addo K., BC Hydro ground motion prediction equations for subduction earthquakes, Earthquake Spectra, Vol. 32(1), 2016, pp. 23-44.

[9] Youngs, R.R., Chiou, S.J., Silva, W.J. and Humphrey, J.R., Strong ground motion attenuation relationships for subduction zone earthquakes, Seismological Research Letters, Vol. *68*(1), 1997, pp.58-73.

[10] Boore D.M. and Atkinson G.M., Ground-Motion Prediction Equations for the Average Horizontal Component of PGA, PGV, and 5%-Damped PSA at Spectral Periods between 0.01 s and 10.0 s, Earthquake Spectra, Earthquake Engineering Research Institute, Vol. 24, No. 1, 2008, pp. 99-138.

[11] Campbell K.W. and Bozorgnia Y., NGA Ground Motion Model for the Geometric Mean Horizontal Component of PGA, PGV, PGD and 5% Damped Linear Elastic Response Spectra for Periods Ranging from 0.01 to 10 s, Earthquake Spectra, Earthquake Engineering Research Institute, Vol. 24, No. 1, 2008, pp. 139-171.

[12] Chiou B. S. J. and Youngs R. R., NGA Model for Average Horizontal Component of Peak Ground Motion and Response Spectra, PEER 2008/09, Pacific Engineering Research Center, College of Engineering, University of California, Berkeley, 2008, pp. 1-94.

[13] Zhao J.X., Irikura K., Zhang J., Fukushima Y., Somerville P.G., Asano A., Ohno Y., Oouchi T., Takahashi T. and Ogawa H., An empirical site-classification method for strong-motion stations in Japan using H/V response spectral ratio, Bulletin of the Seismological Society of America, Vol. 96(3), 2006, pp. 914-925.

[14] Atkinson G.M. and Boore D.M., Empirical ground-motion relations for subduction-zone earthquakes and their application to Cascadia and other regions, Bulletin of the Seismological Society of America, Vol. 93(4), 2003, pp. 1703-1729.

[15] McGuire R.K., Probabilistic Seismic Hazard Analysis and Design Earthquakes, Closing the Loop, Bulletin of The Seismological Society of America, Vol. 85, 5, 1995, pp. 1275-1284.

[16] Leyendecker E.V., Hunt E.J., Frankel A.D. and Rukstales K.S., Development of Maximum Considered Earthquake Ground Motion Maps, Earthquake Spectra, Vol. 16, No.1, 2000, pp. 21-40.

[17] ASCE/SEI 7-10, Minimum Design Loads for Buildings and Other Structures, American Society of Civil Engineers, Virginia, 2010, pp. 1 – 608.

[18] SNI 1726:2012, Tata Cara Perencanaan Ketahanan Gempa untuk Struktur Bangunan Gedung dan Non Gedung (Seismic Resistance Design Code for Buildings and Other Structures), Jakarta, 2012, pp. 1-138.